Tree Physiology 00, 1–12
https://doi.org/10.1093/treephys/tpac120

Research paper

Acclimation of interacting leaf surface traits affects foliar water uptake

Alana R.O. Chin[1,2,4], Paula Guzmán-Delgado[1], Lucy P. Kerhoulas[3] and Maciej A. Zwieniecki[1]

[1]Plant Sciences Department, University of California Davis, Davis, CA 95616, USA; [2]Institute of Integrative Biology, Plant Ecology Group, ETH, Zürich, 8092, Switzerland; [3]Department of Forestry and Wildland Resources, California Polytechnic Institute, Arcata, CA 95521, USA; [4]Corresponding author (alanaroseo@gmail.com)

Received June 3, 2022; accepted October 8, 2022; handling Editor Maurizio Mencuccini

Absorption of water across the surfaces of leaves is an ecologically important aspect of tree physiology. Variation in foliar water uptake capacity depends on environmental conditions when traits associated with the uptake pathway respond to climatic signals. Using a series of experiments, we verify that water enters *Sequoia sempervirens* (D. Don) Endl. leaves by crossing the cuticle, and show that surface-trait acclimation alters the kinetic parameters of foliar water uptake. Under our experimental conditions, the cuticle was the primary pathway for water entry into the leaf. Exposure to climatic variation may induce surface acclimations, such as increased waxiness, that reduce water-film formation over stomata at the expense of dry-season foliar uptake rates. We found that water uptake is negatively associated with the interaction of leaf-surface wax coverage and stomatal density, and provide an accessible protocol to measure these key traits in *Sequoia*. Linking absorptive pathways and trait acclimation to physiological performance can provide a foundation for range-wide or genomic investigations of forest interactions with water and a mechanism-centered means to monitor canopy hydraulic parameters over time.

Keywords: foliar water uptake, functional traits, leaf acclimation, leaf cuticle, leaf wax, rehydration kinetics, *Sequoia*.

Introduction

Foliar water uptake is the capability of terrestrial plants, occurring across taxa and biomes, to absorb water through their leaves (Rundel 1982, Beyer et al. 2005, Guzmán-Delgado et al. 2017, Dawson and Goldsmith 2018, Berry et al. 2019). Capacity for foliar uptake varies not only among and within species, but within the crowns of individual trees, suggesting that uptake potential may be swayed by subtle variation in organ (e.g., leaf) structure and surface physio-chemical properties (Limm and Dawson 2010, Guzmán-Delgado et al. 2016, Kerhoulas *et al.* 2020, Chin et al. 2022*a*). Among the best-studied species capable of absorbing water when leaves are wet, is coast redwood, *Sequoia sempervirens* (D. Don) Endl. (Burgess and Dawson 2004, Simonin et al. 2009, Chin et al. 2022*a* and *b*). The ability to obtain water without relying on soil sources allows *Sequoia* to maintain photosynthetic activity and recover from water stress during dry summers when leaves may become wet due to fog, condensation or occult precipitation (Simonin et al. 2009, Dawson and Goldsmith 2018). Features of leaf surfaces, such as waxiness, create hydraulic resistance that limits foliar uptake in *Sequoia*, and these features can be particularly notable in peripheral shoots where avoiding excessive water accumulation may facilitate wet season photosynthesis (Chin et al. 2022*a*). Many of these leaf-level traits are plastic in their responses to climatic variation, but the impact of their collective environmental responsiveness on foliar uptake is not well understood, especially under conditions inducing simultaneous change in multiple traits.

While leaf traits causing surface hydraulic resistance may alter the way *Sequoia* canopies interact with water, the potential for surface traits in this species to respond to climatic variation is unknown. Such trait variation could have profound impacts on tree performance and forest hydraulics by influencing interception, holding and evaporation of water from canopy surfaces

(Azevedo and Morgan 1974, Holder 2007, Konrad et al. 2012, Schreel and Steppe 2020). *Sequoia* leaves have the broadest range of multivariate within-crown phenotypic plasticity of any conifer measured (Chin and Sillett 2019), but this does not guarantee that uptake capacity is environmentally sensitive independent of height or climatically different sites. Beyond the potential for wide-ranging phenotypic variation within trees, each individual trait has an innate level of developmental plasticity, a 'response repertoire' bounded by the physical, functional and genotypic limits constraining its acclimation (Sultan 2017). While drought appears to increase uptake capacity (Schreel et al. 2019), it is unclear if this is due to trait acclimation or the greater water potential difference. Can climatic conditions alter leaf surface structure and properties to influence water uptake capacity? Evidence from the fern *Polystichum munitum*, which varies in uptake capacity across its range, suggests this may be the case (Limm and Dawson 2010), however experimental work on the malleability of uptake capacity is needed. The exact pathway by which water crosses the leaf surface is unverified in *Sequoia* and conifers in general, thus water might be absorbed through the cuticle, stomata or both, as seen in angiosperm plants (Burgess and Dawson 2004, Eller et al. 2013, Boanares et al. 2018, Berry et al. 2019, Guzmán-Delgado et al. 2021). Lack of knowledge in this basic area makes it difficult to target traits for ecological monitoring or predict climatically induced acclimations in leaf structure that may alter tree-water interactions on regional scales.

Only a limited number of leaf surface-traits have been explored in *Sequoia*, with leaf epidermal anatomy and wettability—the lateral spread of water droplets on leaf surfaces—being mostly uninvestigated. Understanding the importance and developmental stability of leaf traits requires the exploration of uptake parameters across a range of leaf forms, while focusing on a single model species can minimize confounding factors that may hinder interpretation of trait–uptake relationships. Our investigation focuses on *Sequoia*'s peripheral shoots, the majority of the canopy's interceptive surface, because their resistance-causing traits have been associated with maintenance of wet-season photosynthesis at the expense of uptake rate (Chin et al. 2022*a*). We predict that climatic signals, such as temperature, can induce acclimation in key traits that influence foliar water uptake. Further, we hypothesize that if barriers to water entry at the surface of the leaf dominate the series of resistances in the uptake pathway (Guzmán-Delgado et al. 2018, 2021), then superficial traits such as epicuticular wax and stomatal size, not internal anatomical features, will drive variation in the kinetic parameters of foliar water uptake. A structurally dissimilar collection of *Sequoia* peripheral shoots was assembled by broadly manipulating climatic factors during leaf development both within the native range and at a hotter, low-rainfall location outside the native range. Experimental occlusion of stomata and application of fluorescent tracers to leaf surfaces allowed us to ascertain the primary uptake route. Variability of leaf structures associated with both the uptake pathway and capacity allowed us to strategically isolate key traits for future investigations into the impacts of climate change on *Sequoia*'s ability to exploit leaf wetness.

Materials and methods

Maximization of trait diversity

To explore foliar traits enhancing or limiting water uptake capacity and assess their degree of responsiveness to climatic factors, we sought to maximize the diversity of leaf structure. Trait variation was induced in two ways. First, we selected two locations with mature *Sequoia* trees with leaves accessible from ground-level: one a natural forest in the heart of the species' northern range (private land, Humboldt County, CA, 40.8 °N, 124.0 °W) and one a hot, low-rainfall site (with access to landscape irrigation) outside the native range but at a latitude where this species occurs (UC Davis campus, Davis, CA, 38.5 °N, 121.7 °W, Table 1). Second, at each location we placed clear plastic bags around 20 shoot-groups (3–6 shoots per bag) shortly after they completed their expansion (last week of April 2020) and left these bags in place until foliage was harvested at full leaf-hardening (last week of January 2021). For each bag, the closest neighboring shoot with similar characteristics, on the same branch, was labeled as an untreated (control) shoot. Bagging did not appear to influence the coverage of epiphyllic organisms such as algae, which are visible in resin imprints when present (Figure 1C). We obtained preliminary data on the effects of bagging, from 1 week of mid-August monitoring, on the experimental trees within the native range, using HOBO data loggers. We did not find a significant difference in temperature inside bags ($W = 28{,}742$, P-value $= 0.3515$), but within-bag relative humidity (bagged mean $= 90.9 \pm 0.28\%$) was both higher and more consistent than on control shoots (control mean $= 80.2 \pm 0.65\%$, $W = 48{,}155$, P-value $< 2.2\text{e-}16$). In particular, minimum observed humidity values, reached in late afternoon each day, were much higher inside bags (78.8%) than on control shoots (55.4%). The intention behind the bagging was to induce maximum breadth of leaf phenotypic expression; we assume that the bags simultaneously altered a number of latent factors in addition to humidity, evaporative demand and exposure during leaf development. Because our interest for this investigation was in the potential for general environmental malleability of traits related to foliar uptake, we focused on inducing maximum variation in leaf structure, rather than identifying effects of individual climatic factors and their interactions. With this approach, we had four classes of shoots (in-range bagged, in-range untreated, outside-range bagged and outside-range untreated) across which to explore how uptake parameters are influenced by anatomical-structural diversity that we hoped would be induced by exposure to a wide range of climatic conditions (Table 1). Clear plastic bags were placed both in sun and shade on five trees per location

Table 1. Treatments on *Sequoia sempervirens* shoots and their resulting uptake parameters. Temperature and rainfall reflect locational differences during our May 2020 to January 2021 study period (PRISM 2021). For logistic models of the relationship between uptake and time, RMSE can be compared to the asymptote to understand model error. Estimated uptake for 5- and 7-h periods are the predicted total for that timespan from the logistic curves. Maximum rate is the peak value of the first derivative of the logistic curve, and the time to maximum uptake rate is the minutes of fog exposure before the maximum rate is attained. Conductance is calculated by dividing the 7-h estimated uptake by initial water potential before fog exposure. Model asymptote, $\beta 2$, and $\beta 3$ are in units of g m−2 min−1.

Treatment	Maximum temperature (°C)	Rainfall (mm)	*N*	Logistic model asymptote	$\beta 2$	$\beta 3$	RMSE	5-h estimated uptake (g m^{-2})	7-h estimated uptake (g m^{-2})	Maximum uptake rate (g m^{-2} min^{-1})	Time to max uptake (min)	7-h mean conductance (g m^{-2} min^{-1} MPa^{-1})
In-range untreated	26.4	701	15	2.181 ± 2.334	305.87 ± 349.14	147.05 ± 144.41	0.4267	1.0689	1.4938	0.00370	306	0.00156
In-range bagged			17	1.998 ± 0.608	191.43 ± 77.15	86.82 ± 57.55	0.5198	1.5535	1.8643	0.00575	191	0.00190
Outside-range untreated	35.4	126	19	1.906 ± 0.395	152.59 ± 45.45	71.93 ± 38.04	0.4703	1.6881	1.8604	0.00662	153	0.00206
Outside-range bagged			12	2.052 ± 0.459	154.86 ± 42.76	65.35 ± 37.04	0.4185	1.8509	2.0168	0.00785	154	0.00235

(four bags per tree); however, only 1–3 bagged shoots per tree were analyzed due to losses over the growing season. Each bag had a small hole clipped in its lower corner to allow gas exchange and prevent accumulation of transpired water, however, in the mornings condensation was typical inside the bags, indicating a humid environment and some alteration of light availability. Bagged shoots were harvested as part of a larger branchlet so that the untreated shoots adjacent to the bags were also collected whenever available, yielding a total of 63 shoots from the four classes (in-range bagged = 17, in-range untreated = 15, outside-range bagged = 19 and outside-range untreated = 12). In some cases untreated shoots outside the bags were unavailable or had been damaged, leading to uneven sampling.

Measurement of foliar water uptake kinetic parameters

We bench-dried the branchlets with both bagged and untreated shoots attached (1 bag with several shoots per sample) for ∼8 h (this species dries down very slowly), and enclosed them in dark plastic bags in a 5 °C refrigerator for 24 h for equilibration because we have found (Chin et al. 2022*a*) that this prevents further dry-down while allowing all shoots in a cluster to reach the same water potential. We chose to refrigerate our samples because this is much closer to in-range nighttime temperatures than our lab and because, in our experience, they continue to dry-down at room temperature. The following morning, we obtained initial xylem water potential (Ψ) on a shoot from each branchlet with a Scholander pressure chamber; these shoots used for Ψ measurements were then discarded and not used for uptake assessment. Foliar water uptake was measured following the rehydration-kinetics based method of Guzmán-Delgado et al. (2018), where previously weighed shoots with known initial Ψ were placed in a fog chamber in dark conditions (at ∼22 °C) with cut-end sealed with parafilm, and removed at ∼15-min intervals. Following removal, final mass and Ψ were measured for each individual, rehydrated shoot (N = 12–19 per class). Fresh shoots were then carefully dissected into individual leaves and scanned to obtain leaf area before kiln-drying for 48 h at 100 °C for final dry-mass. Shoot-specific water absorption rate (hereafter, 'uptake') was determined as g m^{-2} min^{-1} for principal components analysis (PCA) and trait analyses. It is worth noting that young *Sequoia* shoots, as used here, are entirely covered with leaf bases and lack any bark.

To obtain kinetic parameters representing water uptake in each shoot-class, we plotted the three-parameter logistic relationship of water absorption (g m^{-2}) against time (min), resulting in four curves made up of individual shoot samples, one for each shoot-class (Table 1). We used the standard three-parameter equation:

$$\text{g m}^{-2} = \frac{D}{\left(1 + \frac{\text{minutes}}{C}\right)^{-B}}$$

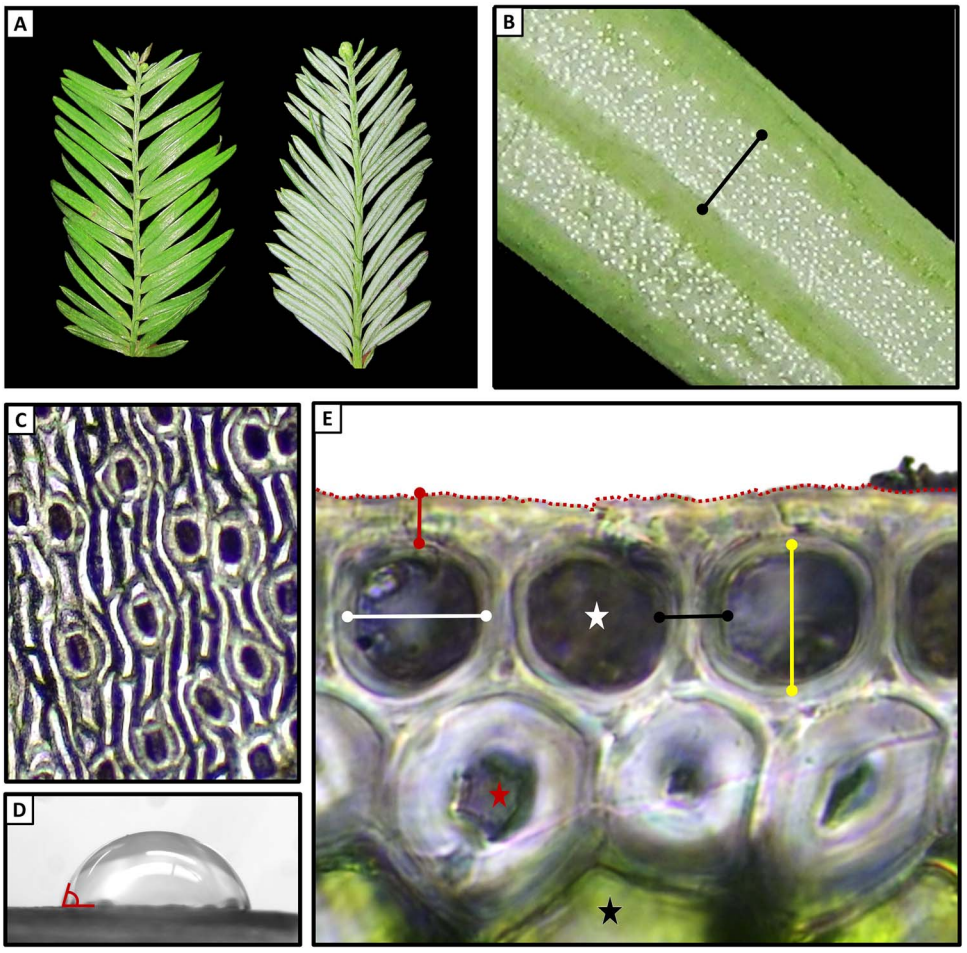

Figure 1. Traits of *Sequoia sempervirens* leaf surfaces and their measurement. (A) The adaxial surface (left) lacks the visible waxes of the abaxial surface (right). (B) Stomata on the abaxial surface, visible as white dots due to presence of wax plugs, occur in two beds on either side of the vein; black spanner = bed width. (C) Stomatal density and guard cell length were measured from resin imprints. (D) Contact angles (shown in red) of water droplets with the leaf surfaces were used to indicate wettability. (E) Cross-section through the adaxial epidermis (40×). White star = epidermal cell, red star = hypodermal cell, black star = mesophyll cell. Dotted red line = surface pathlength used to measure rugosity. Red spanner = cuticle thickness, white spanner = epidermal lumen width, yellow spanner = epidermal lumen height, black spanner = apoplastic thickness. See written descriptions in Table 2.

where D is the asymptote, C is the inflection point and B is the slope. We interpret the root-mean-square error (RMSE) as the overall model error, where and adequately fit (*i.e.*, useful) model has an RMSE less than one half of the estimated asymptote. Logistic curves were used to estimate hydraulic parameters, including maximum rates for rehydration and total uptake over fog-exposure periods up to 7 h. From the first derivative of the logistic curves, we estimated peak surface permeability, hereafter 'maximum uptake rate' (g m^{-2} min^{-1}) and the time to reach this rate (Table 1). We calculated surface conductance for each shoot-class by dividing the 7-h uptake estimate by the initial shoot Ψ.

Measurement of leaf traits

From a subset of sampled branchlets we removed a representative bagged and untreated shoot (N = 6 per shoot-class, Figure 1A). These shoots were used fresh to measure foliar traits representing individual bags or neighboring untreated control-shoots (Table 2), not all bags used had additional shoots remaining for trait measurements, so we chose six branchlets from each location that had paired bagged and un-treated shoots available. Stomatal density, stomatal bed width and guard-cell length were measured from acrylic-resin imprints, surface wax coverage was obtained using color-thresholding of macro images to select wax (Figure 1B and C, see Supplementary data available at *Tree Physiology* Online for detailed wax and stomatal density protocols). Water droplet contact angle was measured from photos of 2-μl droplets of DI water deposited on both the adaxial and abaxial leaf surfaces (five droplets per shoot-class and leaf side) taken at 10× through a sideways microscope (Figure 1D). Epidermal anatomical traits such as lumen diameter and hypodermal thickness were measured from 40× digital images of fresh green cross-sections that were cut with a microtome at a thickness of 10 μm and mounted

Table 2. Traits of *Sequoia sempervirens* leaf surfaces and their developmental plasticity. The 10 traits marked with asterisks (*) were retained in the final PCA and used in multiple regression. CV is the coefficient of variation (SD/mean expressed as a percent), used here as an index of trait developmental plasticity across all treatments. Treatment means are normalized by the full range of observed values for purposes of comparison. Correlations of individual traits with uptake (g H_2O m^{-2} min^{-1}) may be due to their natural allometric relationships to other traits (covariance) and were not used for determination of trait importance, but are provided here as a reference. Traits ordered by plasticity, see visual depictions of trait measurements in Figure 1.

Trait	Definition	Units	Correlation with uptake	Grand mean	CV (%)	Normalized mean (0,1)			
						In-range		Outside-range	
						Untreated	Bagged	Untreated	Bagged
Apoplastic thickness*	Width of the apoplastic space between adaxial epidermal cell lumens	mm	0.21	0.0069	32	0.23	0.26	0.33	0.60
Abaxial wax coverage*	Covering fraction of visible waxes on the abaxial surface	–	−0.65	0.53503	23	0.72	0.57	0.38	0.28
Hypodermal thickness	Anticinal diameter of adaxial hypodermal cells	mm	0.03	0.0262	22	0.45	0.58	0.70	0.50
Stomatal covering fraction	Guard-cell length per area, an index of total pore coverage (abaxial surface)	mm mm^{-2}	0.20	3.6661	22	0.37	0.61	0.49	0.67
Epidermal cell lumen diameter*	Internal diameter of adaxial epidermal cell lumens	mm	−0.32	0.0109	21	0.48	0.68	0.51	0.40
Stomatal bed width*	Width of abaxial stomatal beds	mm	0.63	0.5854	21	0.33	0.18	0.54	0.55
LMA*	Leaf dry mass per fresh area	g m^{-2}	0.45	10.07960666	20	0.66	0.62	0.79	0.73
Stomatal density*	Number of stomata per area on the abaxial surface	Count mm^{-2}	−0.15	112	20	0.37	0.56	0.39	0.58
Adaxial wettability	Water droplet contact angle to leaf adaxial surface, smaller angles indicate greater wettability	Angle	0.14	65.3	20	0.16	0.46	0.19	0.54
Cuticle thickness*	Distance between the innermost edge of the non-lipidic region of pericinal walls of epidermal cells and the adaxial leaf surface	mm	0.21	0.0070	18	0.33	0.51	0.34	0.60
Epidermal cell lumen width*	Internal width of adaxial epidermal cell lumens	mm	−0.40	0.0144	16	0.62	0.71	0.43	0.49
Stomatal bed fraction	Fraction of the abaxial leaf surface occupied by stomatal beds	–	−0.05	0.53	15	0.48	0.43	0.34	0.42
Stomatal guard cell length*	An index of maximum stomatal aperture (abaxial surface)	mm	0.49	0.0328	14	0.46	0.54	0.61	0.58
Abaxial wettability	Water droplet contact angle to leaf abaxial surface, smaller angles indicate greater wettability	Angle	0.16	89.4	10	0.41	0.76	0.53	0.80
Adaxial surface rugosity*	Linear distance per actual surface pathlength, smaller numbers indicate rougher surfaces	–	-0.34	0.9813	2	0.71	0.86	0.72	0.60

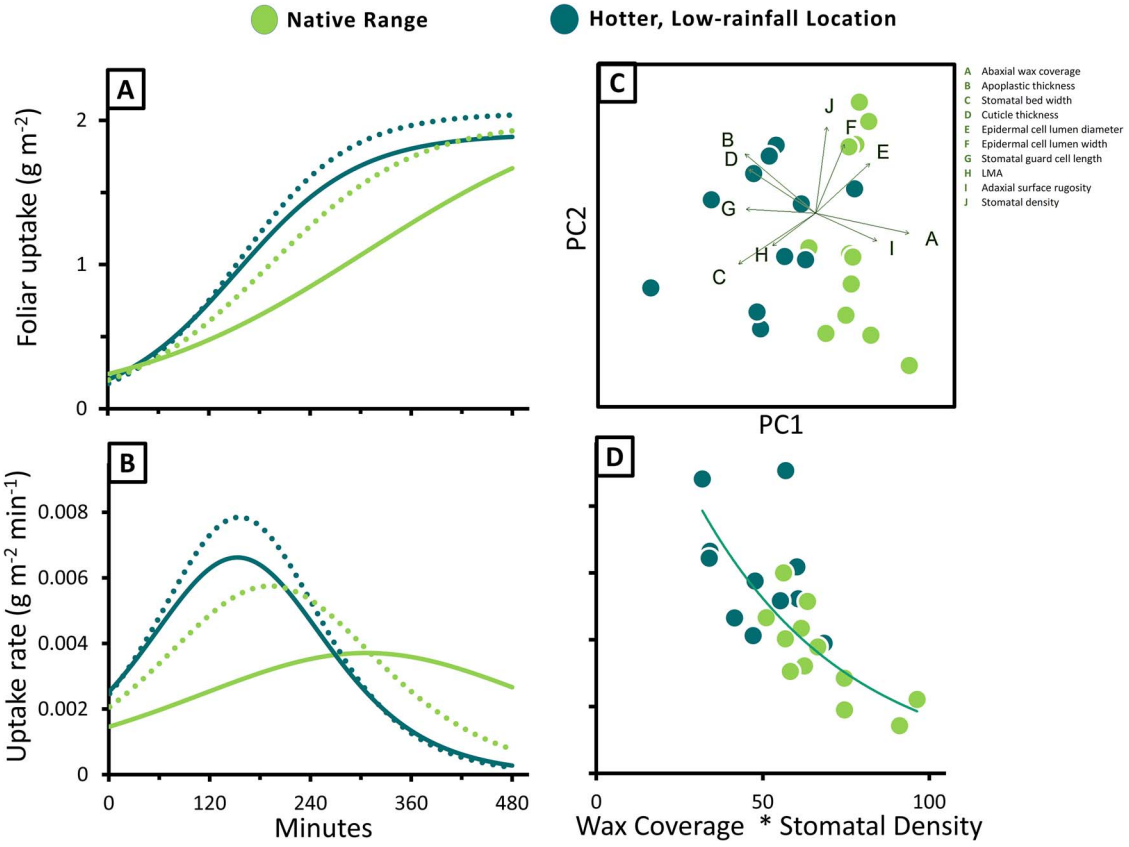

Figure 2. Climate alters leaf uptake capacity and structure. (A and B) Logistic foliar uptake curves (A) for each of our four treatment classes, and their first derivative showing change in rate over time (B), dotted lines indicate bagged samples. (C) PCA of 10 leaf traits shows a clear separation of shoots by location in the first axis (PC1), which is negatively associated with uptake $R^2 = 0.57$. Arrows indicate variable loadings, abaxial wax coverage and stomatal guard cell length heavily loaded on PC1, which separates the sites. (D) The exponential relationship between uptake rate (g m^{-2} min^{-1}) and the interaction of abaxial wax coverage and abaxial stomatal density $R^2 = 0.63$. Shoots with a combination of high wax and high stomatal density have the slowest uptake.

un-stained in water (Figure 1E, Table 2). Due to an error during the photography of surface waxes for one of the in-range control samples, we had a complete set of traits for only 23 out of 24 shoots (see Figure 2).

Contribution of leaf side and cuticle to uptake

To gain further insight into the potential effect of leaf traits on foliar water uptake and the underlying mechanisms driving variability in hydraulic resistance, we quantified the amount of water absorbed by the adaxial versus abaxial leaf surface. The two leaf surfaces differ widely in stomatal density and visible surface-wax coverage. Conveniently, at ground-level it is possible to locate shade-grown *Sequoia* shoots where the adaxial surface is free of stomata, easily verified by the presence of their large, reflective, wax plugs and nail-polish imprints. We painted each individual leaf on a shoot with melted paraffin, to occlude stomata and block the cuticle. Care was taken to cover only the entirely stomata-free adaxial surface, the stomata-covered abaxial surface, or both surfaces with a layer of wax. A set of wax-free shoots were used as a control group. Waxed and control shoots were weighed, had their ends sealed with parafilm, and were then suspended in the fog chamber for 3 h (the approximate time until maximum uptake is reached for these samples) before reweighing. Because small quantities of water clung to imperfections in the waxed surfaces, we subtracted one-half the mean weight-gain of shoots with two waxed surfaces from final weights of all those with single-waxed surfaces, as a correction factor. While a rough correction, it appeared to be reasonable as our mean corrected estimates of abaxial (0.049 mg mm^{-2}) and adaxial (0.145 mg mm^{-2}) uptake summed to a value very near that expected for the whole leaf (whole wax-free leaf = 0.207 mg mm^{-2}).

Additionally, to characterize initial stages of absorption via the cuticle, we applied droplets of the aqueous, exclusively apoplastic, florescent stain, Sulforhodamine B, in a concentration of 0.001% to stomata-free adaxial leaf surfaces for 1 h while leaves remained attached to the shoot, and the shoot retained access to unlimited water through its cut end. We applied stain for only 1 h because longer times resulted in levels of stain absorption that obscured the internal pathway. Droplets were applied to the mid-leaf, to one side of the central vein. Stained leaves were thoroughly rinsed and blotted dry before

immediate sectioning with a microtome using a dry blade and avoiding any exposure of the cut surface to water. Cuts were made adaxial-side down, right-to-left from one leaf corner to the other so that if any un-bound dye was carried by the blade, it would be apparent in the direction of spread. We did not observe any indication of stain spreading as a sectioning artifact. The resulting cross-sections were mounted dry and without coverslip, and photographed alongside identically prepared, unstained leaf-sections from the same shoot at 10×, 20× and 40× under a 535 nm reflected fluorescent light source. We found that 'thick' 20-μm sections provided the best compromise between drying before photography, and image clarity.

Data analysis

The effects and interactions of location and bagging on foliar water uptake were assessed with a permutation-based two-way factorial test, using 5000 runs in the R package asbio(). To avoid multiple univariate comparisons of our 15 traits (see Table 1) to uptake, we began with a multivariate approach to explore the variation of traits among our four shoot-classes as they related to the phenomenon of interest, uptake (g m^{-2} min^{-1}). Using mean shoot values for each bag or sample ($N = 23$), PCA was employed to assess the separation of the four shoot-classes in trait-space and the relationship of the resulting axes (Principal Components, PCs) to uptake. Starting with the complete 15-trait set, we performed an initial PCA, then removed five traits with the most orthogonal relationships to uptake as visualized in the biplot of trait-vectors over the first two PCs. Traits discarded following the first PCA were hypodermal thickness, stomatal covering fraction, stomatal bed fraction, adaxial wettability and abaxial wettability (Table 2). The 10 traits retained for the second PCA round (listed in Table 2) had a mean skewness of 0.15 and mean kurtosis of 0.93, with no individual kurtosis values >2.1, Euclidean distance was used as a measure. To further reduce dimensionality, only the first five resulting PCs, retaining 78% of the trait information, were used to calculate the size and position of the five-dimensional volumes occupied by location and bagging-classes within the shared ordination space, and quantify their overlap with the R package hypervolume().

The 10 traits identified through our initial PCA were used in step-wise multiple linear regression (starting with the saturated model lacking interaction terms), to look for meaningful relationships between the traits measured and parameters representing variation in water absorption. At each step, the lowest-preforming trait was removed and using AICc, R^2 and parameter error were recalculated and used as selection criteria, adding the trait back if its removal did not improve scores. Where the top model had more than one predictor, a model with interaction terms for the predictors was also examined. The individual and interactive effects of location and bagging on the three traits in our top models were assessed collectively with permutation-based factorial tests, and individually with two-sided asymptotic general independence tests in the R package coin(). The relative developmental plasticity (coefficient of variation, SD/mean) of each of the 15 traits was calculated to compare the breadth of their responsiveness. A two-sided asymptotic general independence test was used to compare uptake of leaves with waxed adaxial surfaces to those with waxed abaxial surfaces. PCA was performed in PC-ORD 5 (McCune 1986), and all other analyses and calculations were done in R (R Development Core Team).

Results

Differences in foliar uptake kinetic parameters

For all the shoot classes, the Ψ before rehydration was similar, with a mean value of -2.2 ± 0.07 MPa and no significant differences among treatments ($F = 0.84$, P-value $= 0.49$). The rate of foliar water uptake (g m^{-2} min^{-1}) of individual shoots is dependent on tree location, but not on the effects of bagging, or the interaction of location and bagging (location: $F = 13.15$, P-value $= 0.0014$; bagging: $F = 0.78$, P-value $= 0.3914$; location × bagging: $F = 0.66$, P-value $= 0.4398$). Based on logistic model estimates and driving force changes (i.e., Ψ gradient), there are potentially meaningful differences in estimated rehydration kinetic parameters such as maximum uptake rates, half times and surface hydraulic conductance among the four shoot-classes, such that the outside-range bagged shoots have roughly double the maximum uptake rate of the in-range untreated shoots (Figure 2A and B, Table 1). While these rehydration kinetics curves overlap in some parameters, on the whole their estimated differences appear to be substantial enough to be considered biologically meaningful.

Differences in leaf traits

PCA resulted in one significant axis that retained 27% of the variation in the 10 structural traits used (Table 2), helped explain uptake ($N = 23$, $R^2 = 0.57$) and revealed a distinct separation of samples based on their location (Figure 2C). The hypervolumes defined by the first five PCs, containing 78% of the total variation in the 10 traits, reveal that the two locations (in and out of range) have zero spatial overlap, while bagged and control shoots occupy <10% of the same trait-space. The relative size of their hypervolumes suggests that native-range shoots are the most homogenous group, their relative unitless volumes are: bagged shoots: 11^5, untreated shoots: 13^5, in-range: 5^5, outside-range: 15^5.

Traits determine foliar water uptake parameters

The top two trait-based linear models for uptake both contained abaxial wax coverage and abaxial stomatal density as the predictors, both of which have a negative effect on uptake and are only weakly correlated despite the contribution of plugs to

overall wax coverage (i.e., some low-stomata leaves are quite waxy). The model with the best fit and lowest AICc score is the interaction of wax and stomatal density on the abaxial leaf surface (Model A: uptake $\sim 1 +$ wax * stomatal density; $N = 23$, $R^2 = 0.65$, P-value $= 0.0002$, AICc $= -233.0445$). While the model with an interaction term is much more likely than the next-best additive model (Model B: uptake $\sim 1 +$ wax $+$ stomatal density; $N = 23$, $R^2 = 0.55$, P-value $= 0.0003$, AICc $= -231.0067$, relative likelihood compared with Model A $= 0.25$, Figure 2D), Model A has $>3\times$ the relative error on its parameter estimates, making it a relatively poor predictor and only useful from a phenomenological perspective in understanding the collective importance of those two traits. The mean abaxial wax coverage in each shoot-class is the only trait useable as a predictor for shoot-class maximum uptake ($N = 4$, $R^2 = 0.96$, P-value $= 0.0224$). Moreover, although this trait is potentially positively related to stomatal density in some high-stomata leaves, we cannot be sure of stomatal absorption under our experimental conditions. Apoplastic thickness between epidermal cell lumens appears to have a positive, non-linear effect on these kinetic parameters, suggesting that it may be worthy of further investigation, using a larger number of uptake curves.

Among the two key predictive traits identified through multivariate modeling procedures, abaxial wax coverage is strongly affected by location ($F = 19.57$, P-value $= 0.001$) but not bagging treatment or their interaction. Stomatal density is nearly, but not significantly, dependent on bagging alone ($F = 3.37$, P-value $= 0.083$, Table 2). Apoplastic thickness and abaxial wax coverage had the least developmental plasticity of the 15 traits measured in this study (Table 2).

Confirmation of cuticular water absorption

Under our experimental conditions, water enters *Sequoia* leaves primarily through their stomata-free adaxial side. Shoots with their stomata-covered abaxial surfaces sealed with paraffin absorb ~37 the water over three hours ($N = 4$, mean $= 0.1452$ mg mm^{-2}) compared to leaves with exposed stomata and covered stomata-free adaxial surfaces (mean $= 0.0491$ mg mm^{-2}, $Z = 2.8284$, P-value $= 0.0047$). The sum of the mean single-side uptake values ($N = 5$, 0.1942 mg mm^{-2}) is nearly equal to the mean uptake of unwaxed control leaves ($N = 5$, 0.2071 mg mm^{-2}). Interestingly, the quantity of water absorbed through the abaxial surface, $\sim 25\%$ of total uptake, does not correspond to the generally low-wax spaces between the two stomatal beds and along leaf edges which collectively cover almost half of the abaxial surface (Figure 1B).

After 1-h. of adaxial-surface exposure to Sulforhodamine B, which cannot cross membranes, the stain is visible inside the leaf (Figure 3). Patterns of dye visibility suggest that post-absorption hydraulic transport is both apoplastic and symplastic. A hydraulic path can be traced through the apoplast, from the epidermal site of dye application, directly to the vascular tissue (Figure 3A). At the same time, bright areas of dye concentration in external epidermal and hypodermal walls, indicate that a portion of the water absorbed by leaves enters the symplast at those points, leaving the Sulforhodamine it carries to accumulate outside the cellular membrane (Figure 3B).

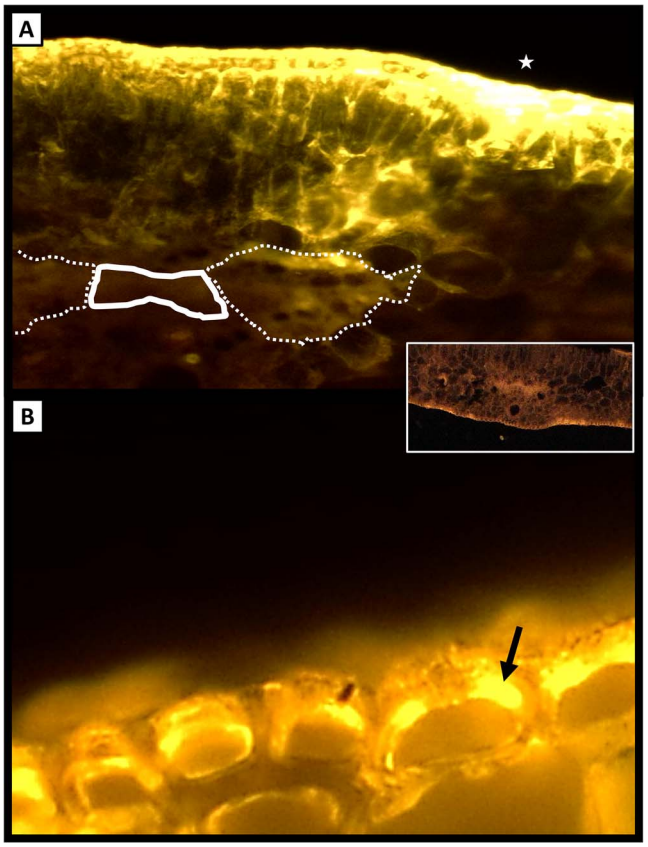

Figure 3. Cuticular pathway of liquid water uptake in *Sequoia sempervirens*. (A) The path of water carrying the fluorescent yellow tracer Sulforhodamine B can be seen traversing a stomata-free region of the adaxial surface. The visibility of dye in the mesophyll and vein conclusively demonstrates an apoplastic pathway from the adaxial site of water application (star) to the vascular tissue (dotted lines = transfusion tissue, white line = xylem). 10×. Inset shows the natural orange autofluorescence of unstained leaves at the same wavelength (535 nm). Autofluorescence is nearly invisible at the low brightness used to photograph the stain. B) Accumulation of dye external to lumens of epidermal cells (bright spots as at arrow) suggests that water enters the symplast at these points, leaving stain outside the cellular membrane. Yellow 'haze' is an artifact of section thickness and stain fluorescence. 40×.

Discussion

Developmental responsiveness of leaf-traits to micro-climatic conditions shapes foliar water uptake capacity in *Sequoia* by altering the kinetics of surface absorption. Leaf traits differ among locations and collectively and individually respond to

the broad variation in climatic stimuli captured in this study (Table 1). In an exciting verification, the key traits associated with uptake variation in our broad trait evaluation, abaxial wax coverage and stomatal density, have been previously implicated as independent causes of hydraulic resistance at the leaf surface using other approaches (Chin et al. 2022*a*). These two traits have relatively high developmental plasticity (Table 2), and their collective effects contribute to the large differences in uptake parameters associated with location and treatment (Figure 2). Negative effects of stomatal density on water absorption could be associated with an increased abaxial wax coverage both on stomatal pores and around stomata; however, it also suggests that, under our experimental conditions, the cuticle is the main pathway for water entry in Sequoia and its permeability may be increased by humidity, such as inside our experimental bags. Our experimental set up is similar to the one described in Guzmán-Delgado et al. (2021) for control leaves (i.e., without chemical modification of stomatal aperture), indicating that, at least under these in vivo conditions, the stomatal pathway is either minimized or excluded (Guzmán-Delgado et al. 2021). As observed in some angiosperm species (Eller et al. 2013, Boanares et al. 2018), the path of water carrying a fluorescent tracer can be seen passing the cuticle in stomata-free portions of the leaf surface (Figure 3A). Our results also highlight the relative importance of the adaxial leaf surface for uptake, which contributed to ~75% of uptake as opposed to the ~50% contribution found in *Prunus dulcis* (Guzmán-Delgado et al. 2021). The adaxial surface has a higher wettability than the abaxial surface leading to an increased contact area between water droplets and the leaf surface itself, potentially increasing the chances for liquid water uptake, though wettability did not appear to positively influence uptake in this study. Additionally, the adaxial leaf surface is free of visible waxes which may indicate that epicuticular waxes contribute to decreasing the permeability of the leaf surface in *Sequoia* (Jetter and Riederer 2016). While there is a distinct apoplastic pathway leading from the leaf surface to the vascular tissue (Figure 3A), an unquantified portion of absorbed water appears to enter the symplast of epidermal and hypodermal cells as indicated by dye accumulation at these sites (Figure 3B) as described by Canny (1993). Unlike *Picea glauca*, where aquaporin upregulation under condensation conditions implies symplastic water transport (Laur and Hacke 2014), *Sequoia* lacks a suberized endodermis that forces water to cross a membrane before reaching the vein—making fully apoplastic transport possible and hinting at family-level differences in conifer hydraulic pathways outside the vascular cylinder. The weak relationship we observed between uptake rate and apoplastic tension, as measured with a pressure chamber ($R^2 = 0.26$, $N = 63$), seemingly contradicts a primarily apoplastic hydraulic path for foliar water uptake. However, potential changes in apoplastic osmotic concentration during the course of water absorption (not measured here) could help explain this surprising lack of correlation. Regardless, while our results suggest both apoplastic and symplastic internal pathways, they only confirm the apoplastic hydraulic route.

Cuticular thickness, wettability and other leaf attributes that respond to environmental variation without meaningfully influencing uptake capacity in *Sequoia*, are equally informative (Table 2). Lack of influence of cuticular thickness on its permeability—despite a cuticular uptake route—has been previously reported, and it may be associated with the heterogeneous distribution of cuticular constituents across the cuticle, including the epicuticular wax layer (Riederer and Schreiber 2001, Fernández et al. 2016, Guzmán-Delgado et al. 2017). In *Sequoia*, the thickest cuticle is present in the highest-uptake bagged outside-range samples, this may be related to the association of cuticular thickness with humidity (Berlyn et al. 1993), which was higher in bags, suggesting this as a target for more detailed work on the induction of leaf surface variability. Interestingly, the least wettable leaves, those where water droplets most readily spread across the leaf surface, were associated with bagged outside-range samples, which had the highest maximum uptake rate (Figure 2B). Neither wettability nor cuticular thickness were related to the coverage of visible waxes. While surface resistance can be largely attributed to visible wax coverage, it is apparently not related to wettability as in some other species (Neinhuis and Barthlott 1997, Koch et al. 2006). Thus the mechanism, by which epicuticular waxes cause hydraulic resistance, might instead involve changes in surface roughness and chemical composition that increase the distance between droplets and the leaf surface (Bhushan and Jung 2008). In this sense, the deposition and further behavior of water droplets on the leaf surface is heterogeneous and varies with both time of exposure to humidity and location within the surface (Roth-Nebelsick et al. 2012, Guzmán-Delgado et al. 2021). Surface waxes may have the potential to be especially responsive to climatic variation because they are one of the few attributes of leaves that can change even in age (Baker 1974). Our results are an interesting contrast to the association of surface waxes with low humidity and high temperature (Koch et al. 2006). Geographic variation in both wettability and water absorption, as observed here, suggests important regional differences in the capacity of forests to intercept and retain rainfall and fog (Azevedo and Morgan 1974, Holder 2007, Konrad et al. 2012).

Potential ecological impacts of altered surface properties can be seen in the striking differences in maximum uptake rate and half-time seen between in-range and outside-range *Sequoia* shoots (Figure 2, Table 1). Shoots grown at the hotter, low-rainfall site outside the species' native range have higher peak uptake rates and reach their maximum uptake in ~2.5 h, approximately double the rate, reached twice as quickly, as

un-manipulated shoots grown in the wet northern range (Figure 2, Table 1). Interestingly, while bagging did not change the half-time in outside-range samples, it moved in-range kinetic parameters closer to the outside-range values (Figure 2, Table 1). Due to differences in conductance and maximum rate we expect that in attached shoots, where whole-tree Ψ would remain relatively low compared with our excised samples, outside-range shoots can absorb more water over any length leaf-wetting event (Table 1). The higher conductance of outside-range shoots indicates that they are better able to exploit brief leaf-wetting events, and that a larger portion of intercepted water would be absorbed rather than dripped to the soil or evaporated from the leaf surface.

As this study was focused on traits and assessment of *Sequoia*'s developmental repertoire under wide-ranging climatic variation, we made no attempt to evaluate the impacts of individual climatic factors. While this is not without value, the effects of individual or small groups of environmental parameters are difficult to interpret in the multi-factor context of site suitability, range limitation or climate change, and do not inform us about change in the forest. Rather, we encourage future *Sequoia* researchers and forestation practitioners to consider and explore the two key traits identified here (visible wax coverage and stomatal density of abaxial leaf surfaces) on a regional and genomic basis, particularly along dry eastern and southern range margins. Toward this end, we provide a detailed protocol for consistently measuring wax coverage and stomatal density, using readily available equipment (see illustrated measurement protocol available as Supplementary data available at *Tree Physiology* Online). As relatively macroscopic features of leaf surfaces, visible wax coverage and stomatal density are particularly usefully traits for ecological monitoring. Ease and low cost of measurement mark these two crucial features as highly suitable for large-scale projects, including those involving volunteers with limited training, thus opening the potential for citizen science. Low developmental stability further suggests the utility of surface wax and stomata for comparison across *Sequoia*'s geographic range and for long-term monitoring.

Acclimation of traits controlling uptake within a single growing season (Table 2, Figure 2), including our observed regional differences in the ability to utilize short-duration leaf-wetting events, indicates that interactions of *Sequoia* forests with atmospheric water are essentially unstable, having the potential to change dramatically with climatic perturbation. Stable isotopes indicate fog interception by *Sequoia* trees almost doubles the annual hydrologic contributions of fog drip to the ecosystem and up to 40 cm of fog drip has been collected in *Sequoia* forests during summer suggesting that it leaf wetness events are available and that fog is readily intercepted by tree crowns (Azevedo and Morgan 1974, Dawson 1998). We expect that, like uptake, these hydrologically important levels of fog drip are also influenced by waxiness and stomatal density of *Sequoia* leaves or by other surface factors, such as wettability, where we observed climate-induced developmental plasticity (Table 2) because these traits would also alter water retention on leaf surfaces. Like the majority of plants in *Sequoia* forests, exploitation of leaf wetness makes critical contributions to plant dry-season survival and ecosystem water cycling worldwide (Breshears et al. 2008, Limm et al. 2009, Eller et al. 2016, Emery 2016, Gotsch et al. 2016, Binks et al. 2019).

Conclusions

The range of developmental plasticity in visible leaf wax coverage and stomatal density we observed indicates potential for climatically driven variation in foliar uptake, while the influence of bagging suggests that uptake capacity may subtlety change with each new crop of leaves. The importance of these two traits points toward the leaf surface as the site of peak resistance in the atmosphere-to-vein hydraulic pathway. Likewise, the key traits identified here both reflect the transcuticular passage of water into *Sequoia* leaves, as verified in this study. Although we cannot rule out a contribution of stomata to foliar water uptake, we present three independently derived pieces of evidence that together confirm cuticular water uptake in *Sequoia*:

(i) Water is absorbed by leaves when the stomata-bearing surface is experimentally occluded.
(ii) Aqueous dye crosses the cuticle in stomata-free portions of the leaf (Figure 3).
(iii) Wax covering the cuticle and stomatal density were collectively associated with low uptake rate, as might be expected if water primarily crossed the cuticle.

Surface wax-cover and stomatal density are easily measured (see Figs S1–S4), and thus hold potential for range-wide investigations or long-term ecological monitoring (see Supplementary Protocol available as Supplementary data at *Tree Physiology* Online). While we expect that surface traits controlling uptake will have phylogenic specificity, detection of uptake-relevant attributes (e.g., hydroids [Gotsch et al. 2016] and trichomes [Ohrui et al. 2007 and Fernández et al. 2014]) in other system-dominating taxa is needed before we can explore their change over time and connect developmental expression to ecological patterns. Isolating key functional traits can be a first step in a conservation-physiology (Seebacher and Franklin 2012) approach to establishing mechanistic and causative links between climate, trait plasticity and ecosystem responsiveness to global change.

Supplementary data

Supplementary data for this article are available at *Tree Physiology* Online.

Acknowledgments

We are grateful to B. Chin and S. Sillett for assistance with the experiment. M. Gilbert and A. McElrone, and two anonymous reviewers provided helpful editorial advice. A.R.O.C. was supported by a Graduate Research Fellowship from US National Science Foundation, P.G.-D. was supported by a Katherine Esau Fellowship from UC Davis.

References

Azevedo J, Morgan DL (1974) Fog precipitation in coastal California forests. Ecology 55:1135–1141.

Baker EA (1974) The influence of environment on leaf wax development in *Brassica oleracea* var. *gemmifera*. New Phytol 73:955–966.

Berlyn GP, Anoruo AO, Vann DR, Johnson AH, Strimbeck GR, Boyce RL, Silver WL (1993) Effects of filtered air and misting treatments on cuticles of red spruce needles on Whiteface Mountain, NY. J Sustain For 1:25–47.

Berry ZC, Emery NC, Gotsch SG, Goldsmith GR (2019) Foliar water uptake: processes, pathways, and integration into plant water budgets. Plant Cell Environ 42:410–423.

Beyer M, Lau S, Knoche M (2005) Studies on water transport through the sweet cherry fruit surface: IX. Comparing permeability in water uptake and transpiration. Planta 220:474–485.

Bhushan B, Jung YC (2008) Wetting, adhesion and friction of superhydrophobic and hydrophilic leaves and fabricated micro/nanopatterned surfaces. J Phys Condens Matter 20:225010. https://doi.org/10.1088/0953-8984/20/22/225010.

Binks O, Mencuccini M, Rowland L et al. (2019) Foliar water uptake in Amazonian trees: evidence and consequences. Glob Chang Biol 25:2678–2690.

Boanares D, Isaias RRMS, de Sousa HC, Kozovits AR (2018) Strategies of leaf water uptake based on anatomical traits. Plant Biol 20:848–856.

Breshears, D.D., McDowell, N.G., Goddard, K.L., Dayem, K.E., Martens, S.N., Meyer, C.W. and Brown, K.M., 2008. Foliar absorption of intercepted rainfall improves woody plant water status most during drought. Ecology, 89(1), pp.41–47.

Burgess SSO, Dawson TE (2004) The contribution of fog to the water relations of *Sequoia sempervirens* (D. Don): foliar uptake and prevention of dehydration. Plant Cell Environ 27:1023–1034.

Canny MJ (1993) Transfusion tissue of pine needles as a site of retrieval of solutes from the transpiration stream. New Phytol 123:227–232.

Chin AR, Sillett SC (2019) Within-crown plasticity in leaf traits among the tallest conifers. Am J Bot 106:174–186.

Dawson TE (1998) Fog in the California redwood forest: ecosystem inputs and use by plants. Oecologia 117:476–485.

Chin AR, Guzmán-Delgado P, Sillett SC, Orozco J, Kramer RD, Kerhoulas LP, Moore ZJ, Reed M, Zwieniecki MA (2022*a*) Shoot dimorphism enables *Sequoia sempervirens* to separate requirements for foliar water uptake and photosynthesis. Am J Bot 109:564–579.

Chin, A.R., Guzmán-Delgado, P., Sillett, S.C., Kerhoulas, L.P., Ambrose, A.R., McElrone, A.R. and Zwieniecki, M.A., 2022*b*. Tracheid buckling buys time, foliar water uptake pays it back: Coordination of leaf structure and function in tall redwood trees. Plant, cell & environment 45(9), pp.2607–2616.

Dawson TE, Goldsmith GR (2018) The value of wet leaves. New Phytol 219:1156–1169.

Eller CB, Lima AL, Oliveira RS (2013) Foliar uptake of fog water and transport belowground alleviates drought effects in the cloud forest tree species, *Drimys brasiliensis* (Winteraceae). New Phytol 199:151–162.

Eller CB, Lima AL, Oliveira RS (2016) Cloud forest trees with higher foliar water uptake capacity and anisohydric behavior are more vulnerable to drought and climate change. New Phytol 211:489–501.

Emery NC (2016) Foliar uptake of fog in coastal California shrub species. Oecologia 182:731–742.

Fernández V, Sancho-Knapik D, Guzmán P et al. (2014) Wettability, polarity, and water absorption of holm oak leaves: effect of leaf side and age. Plant Physiol 166:168–180.

Fernández V, Guzmán-Delgado P, Graça J, Santos S, Gil L (2016) Cuticle structure in relation to chemical composition: re-assessing the prevailing model. Front Plant Sci 7:427. https://doi.org/10.3389/fpls.2016.00427.

Gotsch, S.G., Nadkarni, N. and Amici, A., 2016. The functional roles of epiphytes and arboreal soils in tropical montane cloud forests. Journal of Tropical Ecology 32(5), pp.455–468.

Gotsch SG, Nadkarni N, Darby A, Glunk A, Dix M, Davidson K, Dawson TE (2015) Life in the treetops: ecophysiological strategies of canopy epiphytes in a tropical montane cloud forest. Ecol Monogr 85:393–412.

Guzmán-Delgado P, Graça J, Cabral V, Gil L, Fernández V (2016) The presence of cutan limits the interpretation of cuticular chemistry and structure: *Ficus elastica* leaf as an example. Physiol Plant 157:205–220.

Guzmán-Delgado P, Fernández V, Venturas M, Rodríguez-Calcerrada J, Gil L (2017) Surface properties and physiology of *Ulmus laevis* and *U. minor* samaras: implications for seed development and dispersal. Tree Physiol 37:815–826.

Guzmán-Delgado P, Mason Earles J, Zwieniecki MA (2018) Insight into the physiological role of water absorption via the leaf surface from a rehydration kinetics perspective. Plant Cell Environ 41:1886–1894.

Guzmán-Delgado P, Laca E, Zwieniecki MA (2021) Unraveling foliar water uptake pathways: the contribution of stomata and the cuticle. Plant Cell Environ 44:1728–1740.

Holder CD (2007) Leaf water repellency of species in Guatemala and Colorado (USA) and its significance to forest hydrology studies. J Hydrol 336:147–154.

Jetter R, Riederer M (2016) Localization of the transpiration barrier in the epi-and intracuticular waxes of eight plant species: water transport resistances are associated with fatty acyl rather than alicyclic components. Plant Physiol 170:921–934.

Kerhoulas, L.P., Weisgrau, A.S., Hoeft, E.C. and Kerhoulas, N.J., 2020. Vertical gradients in foliar physiology of tall Picea sitchensis trees. Tree Physiology 40(3), pp.321–332.

Koch K, Hartmann KD, Schreiber L, Barthlott W, Neinhuis C (2006) Influences of air humidity during the cultivation of plants on wax chemical composition, morphology and leaf surface wettability. Environ Exp Bot 56:1–9.

Konrad W, Ebner M, Traiser C, Roth-Nebelsick A (2012) Leaf surface wettability and implications for drop shedding and evaporation from forest canopies. Pure Appl Geophys 169:835–845.

Laur J, Hacke UG (2014) Exploring *Picea glauca* aquaporins in the context of needle water uptake and xylem refilling. New Phytol 203:388–400.

Limm EB, Dawson TE (2010) *Polystichum munitum* (Dryopteridaceae) varies geographically in its capacity to absorb fog water by foliar uptake within the redwood forest ecosystem. Am J Bot 97:1121–1128.

Limm EB, Simonin KA, Bothman AG, Dawson TE (2009) Foliar water uptake: a common water acquisition strategy for plants of the redwood forest. Oecologia 161:449–459.

McCune B (1986) PC-ORD: an integrated system for multivariate analysis of ecological data. Abstracta Botanica 221–225.

Neinhuis C, Barthlott W (1997) Characterization and distribution of water-repellent, self-cleaning plant surfaces. Ann Bot 79:667–677.

Ohrui T, Nobira H, Sakata Y et al. (2007) Foliar trichome-and aquaporin-aided water uptake in a drought-resistant epiphyte *Tillandsia ionantha* Planchon. Planta 227:47–56.

Riederer M, Schreiber L (2001) Protecting against water loss: analysis of the barrier properties of plant cuticles. J Exp Bot 52:2023–2032.

Roth-Nebelsick A, Ebner M, Miranda T et al. (2012) Leaf surface structures enable the endemic Namib desert grass *Stipagrostis sabulicola* to irrigate itself with fog water. J R Soc Interface 9:1965–1974.

Rundel PW (1982) Water uptake by organs other than roots. In: Physiological plant ecology II. Springer, Berlin, Heidelberg, pp 111–134.

Schreel JD, Steppe K (2020) Foliar water uptake in trees: negligible or necessary? Trends Plant Sci 25:590–603.

Schreel JD, von der Crone JS, Kangur O and Steppe, K (2019). Influence of drought on foliar water uptake capacity of temperate tree species. Forests 10:562. https://doi.org/10.3390/f10070562.

Seebacher F, Franklin CE (2012) Determining environmental causes of biological effects: the need for a mechanistic physiological dimension in conservation biology. Philos Trans R Soc B Biol Sci 367:1607–1614.

Simonin KA, Santiago LS, Dawson TE (2009) Fog interception by *Sequoia sempervirens* (D. Don) crowns decouples physiology from soil water deficit. Plant Cell Environ 32:882–892.

Sultan SE (2017) Developmental plasticity: re-conceiving the genotype. Interface Focus 7:201700.